Role of Ground State Structure in Photoinduced Tautomerization in Bifunctional Proton Donor−Acceptor Molecules: 1H-Pyrrolo[3,2-*h*]quinoline and Related Compounds

A. Kyrychenko,[‡,†] J. Herbich,[‡] M. Izydorzak,[‡] F. Wu,[§] R. P. Thummel,[§] and J. Waluk*[,‡]

Contribution from the Institute of Physical Chemistry, Polish Academy of Science, Kasprzaka 44, 01-224 Warsaw, Poland, and Department of Chemistry, University of Houston, Houston, Texas 77204-5641

Received June 1, 1999. Revised Manuscript Received September 27, 1999

Abstract: Spectral, synthetic, and theoretical studies were performed for a family of bifunctional compounds possessing both a hydrogen bond donor (aromatic NH group) and an acceptor (pyridine-type nitrogen atom). The series included 1H-pyrrolo[3,2-*h*]quinoline, 7,8,9,10-tetrahydropyrido[2,3-*a*]carbazole, pyrido[2,3-*a*]-carbazole, dipyrido[2,3-*a*:3′,2′-*i*]carbazole, and 2-(2′pyridyl)indoles. In alcohol solutions, all these compounds reveal the phenomenon of excited state intermolecular double proton transfer, occurring in complexes of the excited chromophore with an alcohol molecule. This process was identified by comparing the fluorescence of the phototautomeric products with the emission of molecules synthesized to serve as chemical models of the tautomeric structures. Detailed investigations demonstrate that the excited state reaction occurs in solvates that, already in the ground state, have an appropriate stoichiometry and structure. These species correspond to 1:1 cyclic, doubly hydrogen bonded complexes with alcohol. Other types of complexes with alcohol were also found, which, upon excitation, undergo deactivation to the ground state via internal conversion. The relative populations of the two forms of alcohol solvates, characterized by different photophysics, vary strongly across the series. The properties of the presently investigated compounds differ from those of a structurally related 7-azaindole and 1-azacarbazole, in which the phototautomerization involves solvent relaxation around the excited chromophore. Molecular dynamics calculations, performed to predict and compare the ground-state structure of 7-azaindole and 1H-pyrrolo[3,2-*h*]quinoline alcohol complexes, allow one to rationalize the observed differences in the excited-state reaction mechanisms for the two kinds of systems.

1. Introduction

Dimers and alcohol complexes of 7-azaindole (**7AI**) reveal, when excited, a biprotonic tautomerization, during which the protons move from the NH groups to the pyridine-type atoms. The process, discovered by Kasha and co-workers in the late sixties,[1] is still attracting much attention.[2−28] **7AI** has become a paradigm in the studies of excited state double proton transfer. Knowledge of the photophysics of this molecule may contribute to the understanding of photoinduced mutagenesis, since **7AI** dimers may be considered as models of DNA base pairs.[29−31]

* Address correspondence to this author.
‡ Polish Academy of Sciences.
† Permanent address: Research Institute for Chemistry, Kharkov State University, 4, Svobody Sq., 310077 Kharkov, Ukraine.
§ University of Houston.

(1) Taylor, C. A.; El-Bayoumi, M. A.; Kasha, M. *Proc. Natl. Acad. Sci. U.S.A.* **1969**, *63*, 253.
(2) Smirnov, A. V.; English, D. S.; Rich, R. L.; Lane, J.; Teyton, L.; Schwabacher, A. W.; Luo, S.; Thornburg, R. W.; Petrich, J. W. *J. Phys. Chem. B* **1997**, *101*, 2758.
(3) Douhal, A.; Kim, S. K.; Zewail, A. H. *Nature* **1995**, *378*, 260.
(4) Douhal, A.; Guallar, V.; Moreno, M.; Lluch, J. M. *Chem. Phys. Lett.* **1996**, *256*, 370.
(5) Chachissvilis, M.; Fiebig, T.; Douhal, A.; Zewail, A. H. *J. Phys. Chem. A* **1998**, *102*, 669.
(6) Folmer, D. E.; Poth, L.; Wisniewski, E. S.; Castleman, A. W., Jr. *Chem. Phys. Lett.* **1998**, *287*, 1.
(7) Takeuchi, S.; Tahara, T. *J. Phys. Chem. A* **1998**, *102*, 7740.
(8) Takeuchi, S.; Tahara, T. *Chem. Phys. Lett.* **1997**, *277*, 340.
(9) Lopez-Martens, R.; Long, P.; Solgadi, D.; Soep, B.; Syage, J.; Millie, Ph. *Chem. Phys. Lett.* **1997**, *273*, 219.
(10) Nakajima, A.; Hirano, M.; Hasumi, R.; Kaya, K.; Watanabe, H.; Carter, C. C.; Williamson, J. M.; Miller, T. A. *J. Phys. Chem. A* **1997**, *101*, 392.
(11) Avouris, P.; Yang, L. L.; El-Bayoumi, M. A. *Photochem. Photobiol.* **1976**, *24*, 211.
(12) McMorrow, D.; Aartsma, T. J. *Chem. Phys. Lett.* **1986**, *125*, 581.
(13) Moog, R. S.; Bovino, S. C.; Simon, J. D. *J. Phys. Chem.* **1988**, *92*, 6545.
(14) Konijnenberg, J.; Huizer, A. H.; Varma, C. A. G. O. *J. Chem. Soc., Faraday Trans. 2* **1988**, *84*, 1163.
(15) Moog, R. S.; Maroncelli, M. *J. Phys. Chem.* **1991**, *95*, 10359.
(16) Herbich, J.; Sepioł, J.; Waluk, J. *J. Mol. Struct.* **1984**, *114*, 329.
(17) Chapman, C. F.; Maroncelli, M. *J. Phys. Chem.* **1992**, *96*, 8430.
(18) Mente, S.; Maroncelli, M. *J. Phys. Chem. A* **1998**, *102*, 3860.
(19) Chen, Y.; Gai, F.; Petrich, J. W. *J. Am. Chem. Soc.* **1993**, *115*, 10158.
(20) Chen, Y.; Gai, F.; Petrich, J. W. *Chem. Phys. Lett*, **1994**, *222*, 329.
(21) Chou, P.-T.; Martinez, M. L.; Cooper, W. C.; Collins, S. T.; McMorrow, D. P.; Kasha, M. *J. Phys. Chem.* **1992**, *96*, 5203.
(22) Chen, Y.; Rich, R. L.; Gai, F.; Petrich, J. W. *J. Phys. Chem.* **1993**, *97*, 1770.
(23) Chang, C.-P.; Wen-Chi, H.; Meng-Shin, K.; Chou, P.-T.; Clements, J. H. *J. Phys. Chem.* **1994**, *98*, 8801.
(24) Chou, P.-T.; Wei, C.-Y.; Chang, C.-P.; Meng-Shin, K. *J. Phys. Chem.* **1995**, *99*, 11994.
(25) Hetherington, W. M., III; Micheels, R. M.; Eisenthal, K. B. *Chem. Phys. Lett.* **1979**, *66*, 230.
(26) Share, P. E.; Sarisky, M. J.; Pereira, M. A.; Repinec, S. T.; Hochstrasser, R. M. *J. Lumin.* **1991**, *48/49*, 204.
(27) Bulska, H.; Chodkowska, A. *J. Am. Chem. Soc.* **1980**, *102*, 3259.
(28) Bulska, H.; Grabowska, A.; Pakuła, B.; Sepioł, J.; Waluk, J.; Wild, U. P. *J. Lumin.* **1984**, *29*, 65.
(29) (a) Löwdin, P. O. *Rev. Mod. Phys.* **1963**, *35*, 724. (b) Löwdin, P. O. *Biopolym. Symp.* **1964**, *1*, 161.
(30) Kasha, M.; Horowitz, P.; El-Bayoumi, M. A. *Molecular Spectroscopy: Modern Research*; Academic Press: New York, 1972; p 287.

10.1021/ja991817z CCC: $18.00
Published on Web 11/19/1999

Considerable progress in the studies of **7AI** has been achieved in recent years, due to the development of supersonic beam techniques, coupled with laser spectrocopy and mass detection. It has been shown that in the gas phase photoreaction in the dimers occurs in a stepwise manner. In the supersonic jet, the first proton is transferred in about 650 fs or even less, while the second proton transfer requires several picoseconds. The exact values depend on the initially excited vibronic level.[3,6]

Information concerning the reaction mechanism in alcohol and water complexes is less complete. It has been recognized that the species which undergoes proton transfer in alcohol solutions is a 1:1 cyclic complex with an alcohol solvent molecule, and that in bulk alcohols such a structure is very rare in the ground state. This has been confirmed by molecular dynamics and Monte Carlo calculations.[18] Therefore, a two-step mechanism seems valid, involving, first, solvent reorganization and, second, proton movement. However, there is still a debate regarding the rate-controlling step.[14−17] An expression $k = k_{PT} \exp(-\Delta G/RT)$ has been proposed, where k_{PT} is the (fast) rate of proton transfer in the system that has achieved a conformation suitable for the reaction and ΔG is the free energy of solvent rearrangement required to achieve such a structure. Using the observation that in properly arranged **7AI** dimers the reaction is very fast, it would seem reasonable to assume that this may also be the case for alcohol complexes. Thus, the rate-limiting step should involve realization of the correct solvation by the alcohol. However, the interpretation of isotopic substitution experiments has led to the proposal that the proton transfer itself may be the rate-determining step.[19,20]

The behavior of **7AI** in water is even more complicated. Contrary to the cases of dimers and alcohol solutions, where dual fluorescence is observed, measurements in water reveal the presence of a single emission, which was assigned to the "normal" form.[11] However, the tautomeric fluorescence may be induced by saturating ethyl ether or *p*-dioxane solutions with water.[21] It was concluded that the **7AI** monohydrate, produced under such conditions, can undergo excited-state proton transfer, and that the reaction is not possible for polyhydrates, prevalent in bulk water.

On the other hand, kinetic studies revealed double exponential decays and growths even in pure water. Two completely different explanations were proposed. Maroncelli and co-workers postulate that phototautomerization in water is qualitatively the same as in alcohols. The process takes about 900 ps and is slow as compared to alcohol solutions. Similarly, a small rate has been found in polyhydroxy solvents such as ethylene glycol and glycerol.[17] On the contrary, Petrich and co-workers claim that in water, only a small fraction, less than 20% of **7AI**, undergoes a rapid (70 ps) tautomerization. The dominant structures correspond to "blocked" complexes, in which the time required for solvent rearrangement leading to the tautomer is estimated to be longer than 10 ns.[22] In another work from the same group, it was postulated that in alcohol solvents there also exists a fraction of complexes which are unable to tautomerize.[20]

Chou and co-workers discovered that the phototautomerization rate can be accelerated by increasing the strength of the hydrogen bond between **7AI** and the complexing partner.[23,24] For instance, in 1:1 complexes between **7AI** and acetic acid, the reaction was so fast that only tautomeric emission could be observed.

There is no doubt that detailed characterization of the structure of the solvates is crucial to understanding the tautomerization mechanism, an extremely difficult task for solution studies. Some help may come from supersonic jet experiments. A cyclic, doubly hydrogen-bonded structure of a 1:1 solvate was proposed based on analysis of the rotational structure of the fluorescence excitation spectra of **7AI**−water complexes.[10] It was also shown that the second and third water molecules in 1:2 and 1:3 complexes are located in the molecular plane of **7AI**.

In view of the above, it seemed instructive to investigate the photophysical characteristics of other bifunctional molecules related to **7AI**. The properties of alcohol solvates of 1-azacarbazole (**1AC**) appear to be similar to those of **7AI**.[32−35] On the other hand, large differences have been observed for a series of bifunctional azaheterocyclic compounds composed of indole, carbazole, or pyrrole hydrogen-bonding donors and of pyridine acceptor units.[36−42] We have shown that the room temperature fluorescence of several methylene-bridged 2-(2′-pyridyl)indoles is strongly quenched in alcohol solutions.[36,37] The quantum yields of fluorescence in alcohols are nearly 2 orders of magnitude lower than in aprotic polar and nonpolar solvents. This difference is observed only for molecules which possess both, the hydrogen bond donor, the NH group, and the hydrogen bond acceptor, the pyridine type nitrogen atom. If one of these groups is modified by methylation on the pyrrolic nitrogen, or removed, e.g., by substituting phenyl for pyridyl, fluorescence becomes equally intense in alcohols as in aprotic solvents. Lowering the temperature leads to the recovery of fluorescence for alcohol solutions of 2-(2′-pyridyl)indoles. In glassy matrices, no significant differences in fluorescence quantum yields are observed for protic and aprotic solvents. The activation energy of the quenching process is correlated with the activation energy of the solvent viscous flow, and remains the same in deuterated alcohols. To interpret these findings, we postulated that the quenching was due to a rapid $S_1 \rightarrow S_0$ internal conversion process, occurring in alcohol solvates which, upon electronic excitation, try to attain a cyclic, doubly hydrogen-bonded arrangement.[37,41]

Other structurally related compounds were found to exhibit very different photophysical characteristics. Dipyrido[2,3-*a*:3′,2′-*i*]carbazole (**DPC**)[40] shows dual fluorescence in alcohols, which is a clear indication of photoinduced tautomerization. In alcohol glasses, the fluorescence intensity is still lower than in aprotic solvents. Remarkably, triple luminescence is observed, consisting of two fluorescence emissions, separated by a phosphorescence band. The excitation spectra prove that the phosphorescence has the same precursor as the higher energy fluorescence. However, the low-energy tautomeric fluorescence must originate from a different ground state species. Such an unusual luminescence pattern was explained by the presence of two different forms of alcohol solvates, of which one only can readily undergo

(31) Goodman, M. F. *Nature* **1995**, *378*, 237.
(32) Chang, C.; Shabestary, N.; El-Bayoumi, M. A. *Chem. Phys. Lett.* **1980**, *75*, 107.
(33) Waluk, J.; Grabowska, A.; Pakuła, B.; Sepioł, J. *J. Phys. Chem.* **1984**, *88*, 1160.
(34) Waluk, J.; Komorowski, S. J.; Herbich, J. *J. Phys. Chem.* **1986**, *90*, 3868.
(35) Fuke, K.; Kaya, K. *J. Phys. Chem.* **1989**, *93*, 614.
(36) Herbich, J.; Rettig, W.; Thummel, R. P.; Waluk, J. *Chem. Phys. Lett.* **1992**, *195*, 556.
(37) Herbich, J.; Hung, C.-Y.; Thummel, R. P.; Waluk, J. *J. Am. Chem. Soc.* **1996**, *118*, 3508.
(38) Herbich, J.; Waluk, J.; Thummel, R. P.; Hung C. Y. *J. Photochem. Photobiol. A*: *Chem.* **1994**, *80*, 157.
(39) Dobkowski, J.; Herbich, J.; Galievsky, V.; Thummel, R. P.; Waluk, J. *Ber. Bunsen-Ges. Phys. Chem.* **1998**, *3*, 469.
(40) Herbich, J.; Dobkowski, J.; Thummel, R. P.; Hegde, V.; Waluk, J. *J. Phys. Chem. A* **1997**, *101*, 5839.
(41) Kyrychenko, A.; Herbich, J.; Izydorzak, M.; Gil, M.; Dobkowski, J.; Wu, F.; Thummel, R. P.; Waluk, J. *Isr. J. Chem.*, in press.
(42) Marks, D.; Zhang, H.; Borowicz, P.; Glasbeek, M.; Waluk, J. In preparation.

Chart 1. Formulas and Acronyms of the Investigated Compounds

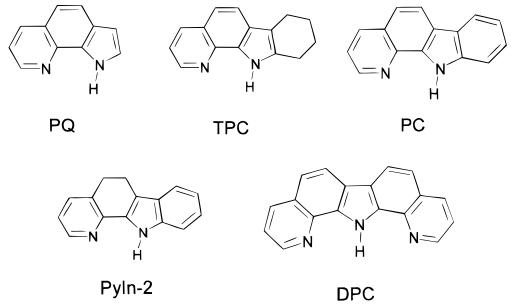

Chart 2. Chemical Models for Indole Tautomers

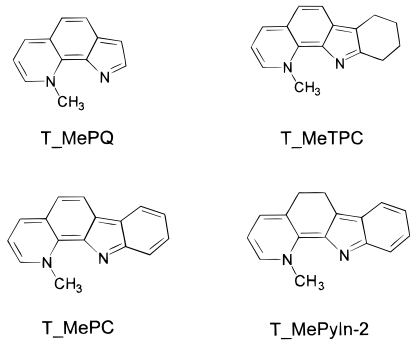

excited state tautomerization. In the other type of complex, an activation energy for the reaction is required. At low temperature, photoinduced proton transfer can only occur in the former type of species. The other structures, "blocked" complexes, emit "normal" fluorescence and "normal" phosphorescence.

The species undergoing fast phototautomerization was attributed to a cyclic, doubly hydrogen-bonded 1:1 complex with alcohol. The other forms were identified as noncyclic 1:*n* complexes, where *n* is the number of alcohol molecules associated with the substrate.

Thus, two different rapid decay channels, internal conversion and double proton transfer, were detected in alcohol solutions. Both depopulation pathways seem to have a common origin: the ability to form cyclic, doubly hydrogen-bonded complexes with alcohols. To understand the mechanisms which make chemically similar molecules conform to one of two different types of photophysical behavior, we have extended our studies to a family of chromophores possessing the same hydrogen bond donor−acceptor structural motif as 2-(2′-pyridyl)indoles and **DPC**. In this work, we compare the properties of previously investigated systems, **PyIn-2** and **DPC**, with those of 1H-pyrrolo[3,2-*h*]quinoline (**PQ**), 7,8,9,10-tetrahydropyrido[2,3-*a*]-carbazole (**TPC**), and pyrido[2,3-*a*]carbazole (**PC**) (Chart 1). Moreover, we have synthesized and studied the photophysics of several indole tautomers (Chart 2), as chemical models for the photochemically generated species: 1-methyl-3,3′-ethenyl-2-(2′-pyrrolenylidene)-1,2-dihydropyridine (**T_MePQ**), 1-methyl-4′,5′,6′,7′-tetrahydro-3,3′-ethenyl-2-(2′-indolenylidene)-1,2-dihydropyridine (**T_MeTPC**), 1-methyl-3,3′-dimethene-2-(2′-indolenylidene)-1,2-dihydropyridine (**T_MePC**), and 1-methyl-3,3′-dimethylene-2-(2′-indolenylidene)-1,2-dihydropyridine (**T_MePyIn-2**). Knowledge of the photophysical parameters of these model compounds is crucial for understanding the phototautomerization mechanism. First, such knowledge enables an unambiguous assignment of the low-energy fluorescence to the phototautomerizing species. Second, it allows one to determine the fraction of the ground-state population that undergoes excited-state proton transfer, a basic feature in testing various models for the excited-state reaction.

The results allow us to describe the behavior of all the systems studied in terms of a general model. Its starting point is the ground-state equilibrium between cyclic and noncyclic alcohol complexes. If the former type of solvate is dominant, phototautomerization cannot be stopped even at low temperature. On the contrary, if the noncyclic species predominate, an energy barrier exists, associated with solvent reorganization. For such a case, phototautomerization can be blocked by lowering the temperature or increasing the solvent viscosity. An efficient radiationless deactivation channel was located on the excited-state energy surface, along the path leading from noncyclic to cyclic species. Therefore, the excitation of a noncyclic structure leads to $S_1 \rightarrow S_0$ internal conversion that effectively competes with tautomerization.

2. Experimental and Computational Details

Syntheses and purification procedures of 2-(2′-pyridyl)indoles,[43] dipyrido[2,3-*a*:3′,2′-*i*]carbazole (**DPC**),[40] 1H-pyrrolo[3,2-*h*]quinoline (**PQ**),[44] 7,8,9,10-tetrahydropyrido-[2,3-*a*]carbazole (**TPC**),[45] and pyrido-[2,3-*a*]carbazole (**PC**,[45] and the models of tautomeric forms[44,45] were described elsewhere.

Electronic absorption spectra were recorded on a Shimadzu UV 3100 spectrophotometer, equipped with variable-temperature chambers, allowing temperature control between 88 and 333 K with accuracy of ±1 K. Fluorescence spectra were measured either on Jasny spectrofluorimeters[46] or on an Edinburgh Instruments FS900 steady-state fluorimeter. The former instruments were used for studies of temperature dependence of luminescence, with a temperature stability of ±2 K. As a quantum yield standard, we used either quinine sulfate in 0.1 N H_2SO_4[47a] ($\varphi_{fl} = 0.51$) or a water solution of $[Ru(bpy)_3](ClO_4)_2$ ($\varphi_{fl} = 0.042$).[47b] Low-energy fluorescence bands were recorded twice to eliminate radiation due to interference from the second order of the grating. First, the whole spectral range was scanned. Then, a blue cutoff filter was used on the emission side and the low-energy band was separately recorded.

Fluorescence decays were measured on an Edinburgh Instruments FL900 fluorescence lifetime spectrometer. Some decays were also recorded on an instrument with higher temporal resolution, using a picosecond TCSPC system at the Ultrafast Laser Spectroscopy Laboratory at the A. Mickiewicz University, Poznań, Poland. The details of this apparatus are given in ref 48. All solvents were spectral grade.

The measurements in alcohols were done using methanol, ethanol, 1-propanol, and 1-butanol. The results of investigations of the influence of alcoholic solvent properties on the photophysics of the solvates will be reported separately.[42]

Excited-state energies and effective valence electron potentials[49−51] were computed using the INDO/S method.[52] Up to 460 lowest singly excited configurations were taken into account in the CI procedure. Ground-state geometries and energies were obtained by ab initio calculations, using the RHF or DFT(B3LYP) models and the 6-31+G-(d,p) basis set, as implemented in the Gaussian 98 suite of programs.[53] Molecular dynamics studies were performed with the GROMOS96 program with the 43A1 force field,[54] using the electronic densities on

(43) Thummel, R. P.; Hedge, V. *J. Org. Chem.* **1989**, *54*, 1720.
(44) Wu, F.; Thummel, R. P. Submitted for publication.
(45) Wu, F.; Hardesty, J.; Thummel, V. *J. Org. Chem.* **1998**, *63*, 4055.
(46) (a) Jasny, J. *J. Lumin.* **1978**, *17*, 149. (b) Jasny, J.; Waluk, J. *Rev. Sci. Instrum.* **1998**, *69*, 2242.
(47) (a) Velapoldi, R. A. *Natl. Bur. Stand. 378, Proc. Conf. NBS*; Gaithersburg 1972; p 231. (b) Caspar, J. V.; Meyer, T. J. *J. Am. Chem. Soc.* **1983**, *105*, 5583.
(48) Dobek, K.; Karolczak, J.; Komar, D.; Kubicki, J.; Szymański, M.; Wróżowa, T.; Ziółek, M. *Optica Appl.* **1998**, *28* (No. 3), 201.
(49) Spanget-Larsen, J. *J. Chem. Soc., Perkin Trans. 2* **1985**, 417.
(50) Spanget-Larsen, J. *J. Phys. Org. Chem.* **1995**, *8*, 496.
(51) Waluk, J.; Rettig, W.; Spanget-Larsen, J. *J. Phys. Chem.* **1988**, *92*, 6930.
(52) Ridley, J. E.; Zerner, M. Z. *Theor. Chim. Acta* **1973**, *32*, 111.

atoms obtained during ab initio geometry optimizations. These charges were calculated from fits of the molecular electrostatic potentials determined by the ground-state wave functions. A rigid all-atom model was used for the solute molecules, with each atom treated as a separate charge group. This required some adjustment of the standard GROMOS96 force field parameters (bond lengths and angles) to retain the ab initio optimized geometry. The standard Lennard-Jones parameters were taken from the GROMOS96 force field without changes. The solvent parameters for methanol were taken from the GROMOS96 library. For *n*-hexane, the bond lengths and angles were adapted from ref 55, allowing the possibility of internal rotations around CH_3-CH_2 and CH_2-CH_2 bonds, modeled with a standard GROMOS96 torsional potential energy function. The solute molecules were placed in the center of a cubic box, filled with the solvent at an equilibrium distribution. Solvent molecules lying outside the box or overlapping with solute atoms (solute−solvent distance <0.23 Å) were removed. The final systems included 116 and 216 solvent molecules for *n*-hexane and methanol, respectively. For each system, the energy minimization was first performed to obtain the starting structure for molecular dynamic simulations. This was followed by a 50 ps simulation for solvent equilibration at constant temperature and volume, and another 50 ps at constant temperature and pressure. The whole system was then allowed to relax for 100 ps, after which the trajectories, saved every 10 fs, were collected for 500 ps. All simulations were performed using a periodic boundary condition at a temperature of 300 K and pressure of 1 atm. The temperature and pressure were maintained by weak coupling to an external bath,[56] using a relaxation time of 0.1 and 0.5 ps, respectively. The bond lengths were constrained using the SHAKE algorithm[57] with relative geometry precision of 10^{-4}. The integration time step was 0.5 fs. A cutoff radius of 1.1 Å was used for nonbonded interactions, which were calculated at each time step using a charge-group pair list that was updated every 20 time steps.

3. Results and Discussion

Figure 1 presents the electronic absorption spectra of **PQ**, **TPC**, **PC**, and **PyIn-2** as well as the absorption spectra of the corresponding tautomeric model compounds. The absorption patterns vary, reflecting the extent of the π-electron chromophore. Generally, the lowest energy absorption bands in the "normal" forms are insensitive to changes in solvent polarity. The lowest energy electronic transitions in the tautomer models are strongly red-shifted with respect to those observed in the "normal" forms. These transitions undergo considerable blue shifts in more polar solvents. As an example, the absorption spectra of **T_MePQ** in various solvents are presented in Figure 2. The increase of transition energy with solvent polarity indicates that the dipole moments in the tautomeric forms decrease upon $S_1 \leftarrow S_0$ excitation. This was indeed confirmed by calculation (Table 1), which also reproduced very well the large red shifts of the first electronic absorption band of the tautomeric model species (cf. Table 3).

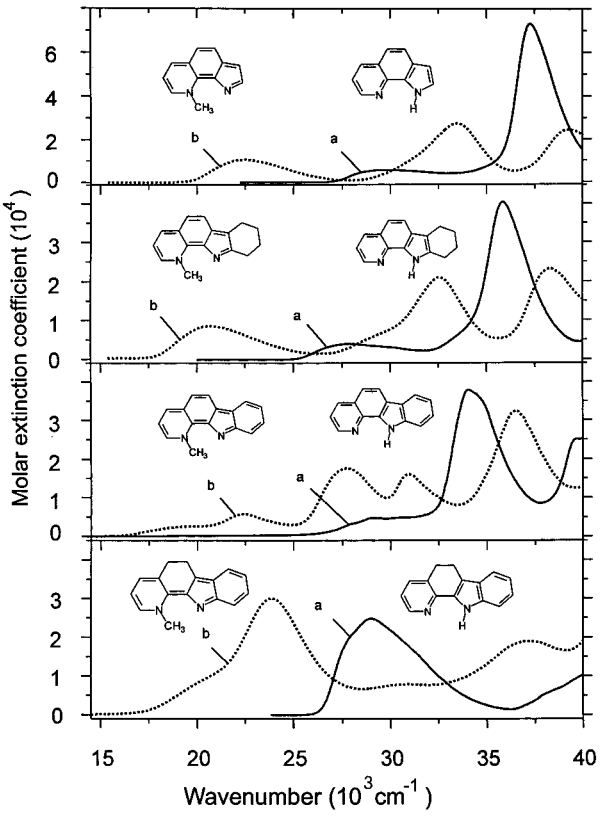

Figure 1. Absorption spectra of **PQ**, **TPC**, **PC** and **PyIn-2** (solid lines, a) and of the corresponding tautomeric model structures (dashed lines, b). The spectra were recorded in 1-butanol at 293 K.

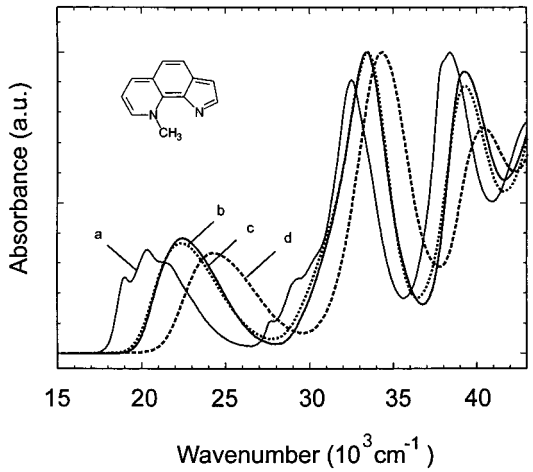

Figure 2. Absorption spectra of **T_MePQ** in *n*-hexane (solid line, a), acetonitrile (dotted line, b), 1-butanol (solid line, c), and water (dashed line, d) at 293 K. The curves were normalized to the highest peak.

Fluorescence spectra are shown in Figure 3. Table 2 contains photophysical characteristics obtained in various types of solvents. All the compounds reveal similar response to a change from an aprotic to a protic solvent. Fluorescence intensities which are quite high in both polar and nonpolar aprotic media become very weak in alcohols. Moreover, dual fluorescence is observed in alcohol solutions. In addition to the "normal" fluorescence (F_1), similar in shape and position to the emission observed in polar aprotic solvents, another band (F_2) appears at much lower energy. The shifts between the maxima of the two emissions vary from 8000 cm^{-1} in **TPC** to 10650 cm^{-1} in

(53) *Gaussian 98, Revision A.6*; Frisch, M. J.; Trucks, G. W.; Schlegel, H. B.; Scuseria, G. E.; Robb, M. A.; Cheeseman, J. R.; Zakrzewski, V. G.; Montgomery, J. A., Jr.; Stratmann, R. E.; Burant, J. C.; Dapprich, S.; Millam, J. M.; Daniels, A. D.; Kudin, K. N.; Strain, M. C.; Farkas, O.; Tomasi, J.; Barone, V.; Cossi, M.; Cammi, R.; Mennucci, B.; Pomelli, C.; Adamo, C.; Clifford, S.; Ochterski, J.; Petersson, G. A.; Ayala, P. Y.; Cui, Q.; Morokuma, K.; Malick, D. K.; Rabuck, A. D.; Raghavachari, K.; Foresman, J. B.; Cioslowski, J.; Ortiz, J. V.; Stefanov, B. B.; Liu, G.; Liashenko, A.; Piskorz, P.; Komaromi, I.; Gomperts, R.; Martin, R. L.; Fox, D. J.; Keith, T.; Al-Laham, M. A.; Peng, C. Y.; Nanayakkara, A.; Gonzalez, C.; Challacombe, M.; Gill, P. M. W.; Johnson, B.; Chen, W.; Wong, M. W.; Andres, J. L.; Gonzalez, C.; Head-Gordon, M.; Replogle, E. S.; Pople, J. A. Gaussian, Inc.: Pittsburgh, PA, 1998.

(54) Van Gunsteren, W. F.; Billeter, S. R.; Eising, A. A.; Hünenberger, P. H.; Krüger, P.; Mark, A. E.; Scott, W. R. P.; Tironi, I. G. *Biomolecular Simulation: The GROMOS96 Manual and User Guide*; Biomos B.V.: Zürich, Groningen, 1996.

(55) Jorgensen, W. L.; Modura, J. D.; Carol, J. S. *J. Am. Chem. Soc.* **1984**, *106*, 6, 6638.

(56) Berendsen, H. J. C.; Pastma, J. P. M.; van Gunsteren, W. F.; Nola, A.; Haak, J. R. *J. Chem. Phys.* **1984**, *81*, 3684.

(57) Ryckaert, J. P.; Ciccott, G.; Berendsen, H. J. C. *J. Comput. Phys.* **1977**, *23*, 327.

Table 1. The INDO/S Calculated Energy Values of the Lowest Excited Singlet States, Oscillator Strengths, Dipole Moments, and the Changes of the Effective Valence Electron Potentials (EVEP) upon $S_1 \leftarrow S_0$ Excitation

	$E(S_1)^a$ [10^3 cm^{-1}]	$\mu(S_0)$ [D]	$\mu(S_1$ [D]	$W^N(S_0)^b$ [eV]	$\Delta W^N(S_1)^c$ [eV]	$W^{NH}(S_0)^d$ [eV]	$\Delta W^{NH}(S_1)$ [eV]	$W^N(S_0)^e$ [eV]	$\Delta W^N(S_1)$ [eV]
PQ	29.3 (0.031)	1.14	2.60	−11.59	0.64	−5.65	−0.45		
T_MePQ	20.2 (0.255)	5.74	1.28					−10.31	1.54
TPC	28.4 (0.067)	0.80	4.88	−11.52	0.95	−5.59	−0.58		
T_MeTPC	19.6 (0.337)	4.70	2.47					−10.34	1.42
PC	28.3 (0.010)	2.15	1.19	−11.68	0.44	−5.57	−0.43		
T_MePC	15.2 (0.061)	8.92	4.15					−10.09	2.15
PyIn-2	29.9 (0.804)	2.46	2.55	−11.74	1.14	−5.57	−0.26		
T_MePyIn-2	18.5 (0.426)	7.19	3.44					−10.10	1.87

[a] Oscillator strengths in parentheses. [b] EVEP for the pyridine type nitrogen atom. [c] $\Delta W^N(S_1) = W^N(S_1) - W^N(S_0)$. [d] $W^{NH} = (1/2)(W^N + W^H)$. [e] deprotonated pyrrole nitrogen in the tautomer model.

Table 2. Photophysical Parameters of **PQ**, **TPC**, **PC**, and **PyIn-2**: Absorption ($\tilde{\nu}_{abs}$) and Fluorescence ($\tilde{\nu}_{fl}$) Maxima, Fluorescence Quantum Yields (ϕ_{fl}), and Decay Times (τ_{fl})

solvent	$\tilde{\nu}_{abs}$ [cm^{-1}]	$\tilde{\nu}_{fl}$ [cm^{-1}]	ϕ_{fl}[a]	τ_{fl}[b] [ps]
		PQ		
n-hexane	28900	27300	0.25	6300
acetonitrile	30500	25850	0.16	4300
1-butanol F_1	29700	26000	0.0013	60 ± 20[c,d]
1-butanol F_2		17200	0.0008	290 ± 20[c]
		TPC		
n-hexane	28750	25450	0.26	6700
acetonitrile	28650	23000	0.17	5000
1-butanol F_1	27800	23850	0.0006	60 ± 20[c,d]
1-butanol F_2		15850	0.0017	190 ± 20[c]
		PC		
n-hexane	29250	25600	0.32	10100
acetonitrile	29500	23200	0.15	7100
1-butanol F_1	29150	23600	0.0015	60 ± 20[c,d]
1-butanol F_2		14400	0.0002	60 ± 10[c]
		PyIn-2		
n-hexane	29600	26350	0.50	1300
acetonitrile	29650	25700	0.38	1800
1-butanol F_1	29050	25550	0.009	<200
1-butanol F_2		14900	0.0003	<200

[a] Estimated error: ±20% for $\phi_{fl} > 0.01$ and ±40−50% for $\phi_{fl} < 0.01$. [b] Estimated error: ±200 ps. [c] Measured with higher time resolution (single picoseconds). [d] Biexponential decay, the longer component reported.

PyIn-2 (cf. Table 2). The spectral locations and shapes of the low-energy emissions coincide nearly exactly with the fluorescence recorded for the tautomeric model structures, for which the photophysical parameters are presented in Table 3. Also, the decay times are quite similar. These findings leave no doubt that the low-energy fluorescence originates from the tautomeric species, obtained as a result of a double proton-transfer reaction occurring in complexes of the photoexcited chromophore with alcohol. Such behavior is analogous to that found at room temperature for **7AI**[1,11] and **1AC**.[34] For **DPC**, we have already postulated the occurrence of this process in alcohol complexes.[40] On the other hand, in our previous studies of pyridylindoles,[36,37] we were not able to detect the extremely weak tautomeric emission in these molecules. The present studies made this detection possible due to the higher sensitivity of the instrument. Fluorescence excitation spectra of both bands agree with the absorption, as shown in Figure 4 for **PyIn-2**. The detection of phototautomerization for all the molecules studied implies that differences in their photophysical behavior are merely quantitative and thus a common model may be developed to describe the whole set.

The driving force for the excited-state proton transfer is the electron density redistribution occurring upon excitation. This redistribution leads to an increase in the excited-state pK_a of the proton acceptor, a decrease in the excited-state pK_a of the proton donor, or a combination of both. Changes of pK_a in the excited state can be obtained from the "Förster cycle",[58,59] employing the formula:

$$\Delta pK_a = pK_a^* - pK_a^G \approx -0.00207(\tilde{\nu}_{00}^A - \tilde{\nu}_{00}^B) \quad (1)$$

where pK_a* and pK_a^G denote values in the excited and ground state, respectively; the electronic transition energies in the acid ($\tilde{\nu}_{00}^A$) and base ($\tilde{\nu}_{00}^B$) forms are expressed in wavenumbers.

This procedure was applied using the spectra of neutral and protonated molecules, as shown for **PQ** in Figure 5. From the absorption and fluorescence of the neutral and protonated species, the 0−0 transitions of both forms can be estimated, yielding the change in pK_a upon $S_1 \leftarrow S_0$ excitation for protonation on the pyridine nitrogen atom: $\Delta pK_a(N) = +9.6$. Since it was difficult to find conditions for deprotonating the NH group in the ground state, the analogous pK_a changes for this group were not determined. However, it was possible to evaluate, somewhat less accurately, the pK_a change for the deprotonation of the NH group in the singly protonated species using the shift in the fluorescence maxima corresponding to the tautomer and that of the protonated monocation. This shift for **PQ** resulted in $\Delta pK_a(NH)) = -6$. The values for the other compounds are given in Table 4. It can be seen that large pK_a

Table 3. Photophysical Parameters for the Tautomer Models of **PQ**, **TPC**, **PC**, and **PyIn-2** (See Table 2 for Details)

solvent	$\tilde{\nu}_{abs}$ [cm^{-1}]	$\tilde{\nu}_{fl}$ [cm^{-1}]	ϕ_{fl}[a]	τ_{fl}[b] [ps]
		T_MePQ		
n-hexane	20350	15800	0.0013	<700
acetonitrile	22420	16150	0.0011	<600
1-butanol	22450	16650	0.0024	350 ± 20[c]
water	24240	16750	0.0009	<700
		T_MeTPC		
n-hexane	18800	15600	0.0010	<200
acetonitrile	20550	16000	0.0014	<400
1-butanol	20725	16650	0.0036	200 ± 20[c]
water	22750	16800	0.0032	<700
		T_MePC		
acetonitrile	19270	14600	0.0003	<600
1-butanol	19420	14150	0.0006	60 ± 10[c]
water	20830	14600	0.0001	<500
		T_MePyIn-2		
acetonitrile	20160	14500	0.0001	<200
1-butanol	19880	14900	0.0005	<200

[a] Estimated error: ±40−50%. [b] Estimated error: ±200 ps. [c] Measured with higher time resolution (single picoseconds).

(58) Förster, T. *Z. Elektrochem. Ber. Bunsen-Ges. physik. Chem.* **1950**, *54*, 42.

(59) Grabowski, Z. R.; Grabowska, A. *Z. phys. Chem. NF* **1976**, *101*, 197.

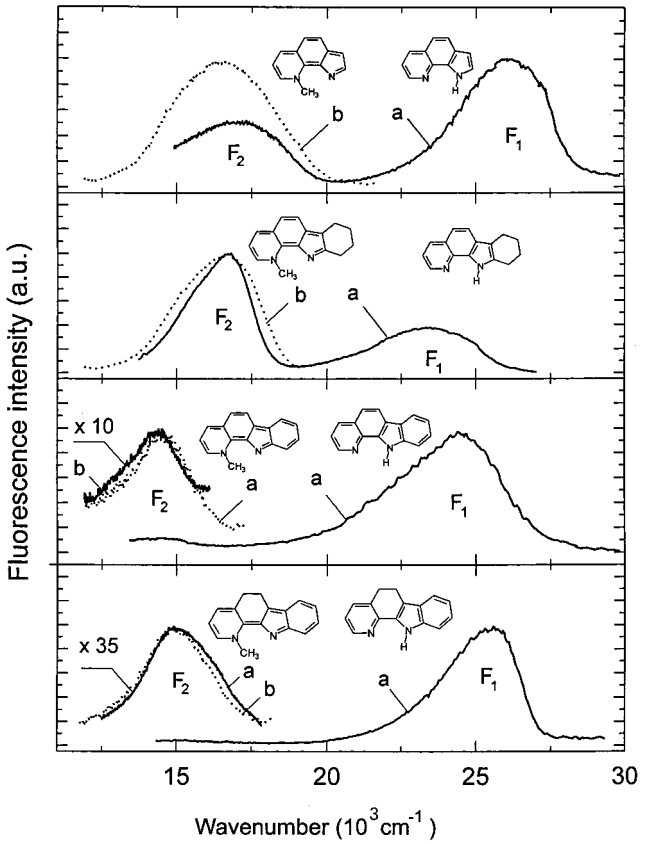

Figure 3. Fluorescence of **PQ**, **TPC**, **PC**, and **PyIn-2** (solid lines, a) and of the corresponding tautomeric model structures (dotted lines, b). The spectra were recorded in 1-butanol at 293 K.

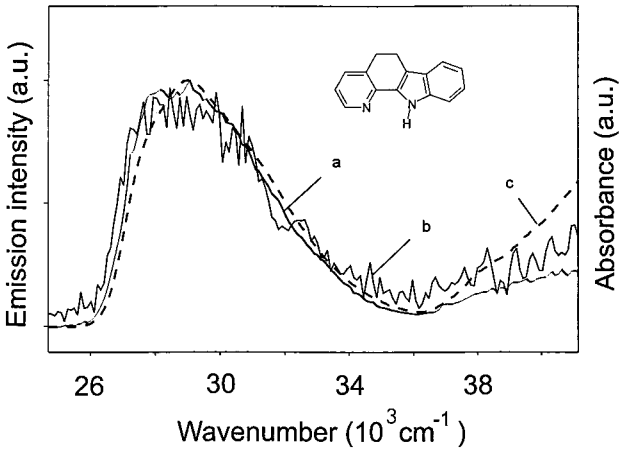

Figure 4. Excitation spectra of both fluorescence bands of **PyIn-2** in 1-butanol at 293 K. The emission intensity of the F_1 band was monitored at 410 nm (a) and the intensity of the F_2 band at 680 nm (b). The absorption curve is given for comparison (c).

changes occur upon excitation, clearly favoring proton transfer, since the pyridine nitrogen atom becomes more basic than the nitrogen of the NH group. Changes in acid−base behavior can also be predicted by calculation. We have shown previously that the effective valence electron potentials,[49,50] quantities that take into account the electronic distribution in the whole molecule, can be used as reactivity indices.[37,51] Table 1 contains the values of changes in these potentials for the lowest excited singlet state, computed for the N and NH centers. The less negative values of the potential indicate higher basicity. For all the compounds studied, a large increase in the basicity of the pyridine nitrogen, as well as a concomitant increase in the NH

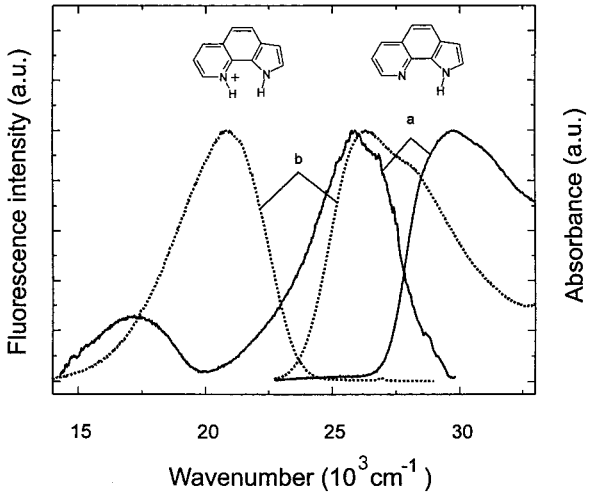

Figure 5. Electronic absorption and fluorescence spectra of neutral (solid lines, a) and protonated (dashed lines, b) **PQ** recorded in 1-butanol at 293 K. Protonation was achieved by adding a small amount (10^{-2} M) of HNO_3.

Table 4. Ground State pK_a Values and pK_a Changes in the Lowest Excited Singlet State for Protonation on the Pyridine Nitrogen Atom (ΔpK_a(N)) and for Deprotonation of the NH Group (ΔpK_a(NH) in the Singly Protonated Species[a]

	pK_a	ΔpK_a(N)	ΔpK_a(NH)
PQ	4.5 ± 0.2	9.6 ± 1	-6.0 ± 1
TPC	4.2 ± 0.2	9.1 ± 1	-5.1 ± 1
PC	3.9 ± 0.1	10.2 ± 1	-4.3 ± 1
PyIn-2	4.4 ± 0.2	12.2 ± 2.5	-4.9 ± 1

[a]All the measurements were done in water solutions.

group acidity, is predicted. Comparison with the experimental results presented in Table 4 shows that the predicted changes in acid−base behavior do indeed occur in all the systems studied.

In previous work, we have demonstrated the formation of specific complexes of bridged pyridylindoles[37] and **DPC**[40] with alcohol molecules. Titration of solutions of pyridylindoles in a nonpolar solvent with alcohol (in concentrations low enough to prevent the formation of alcohol oligomers) was accompanied by changes in the absorption spectra, from which equilibrium constants could be determined. It was found that at low alcohol concentrations, 1:1 complexes were formed. In bulk alcohol, complexes of higher order, 1:n with $n \geq 2$, were dominant. For **DPC**, however, the situation was different. The 1:1 complexes were found to be in large excess. Moreover, from the fact that tautomeric emission was observed even in low-temperature rigid alcohol glasses, we deduced the cyclic geometry of the 1:1 solvates.

Figure 6 presents the results of adding 1-butanol to a solution of **PQ** in a nonpolar solvent, *n*-hexane. Spectral changes are seen both in absorption and in emission. In the absorption spectra, isosbestic points are observed. In emission, the decrease of the "normal" fluorescence is accompanied by the appearance, at lower energies, of the tautomeric band. Assuming a presence of two species, a "bare" molecule and a complex with alcohol, one can determine the equilibrium constant independently from the absorption and emission measurements. The absorption data yielded for **PQ** the value of $K = 180$ M^{-1} and $n = 1.01 \pm 0.02$ for the number of molecules participating in the complex (see insert to Figure 6). The fluorescence data gave $K = 115$ M^{-1}. The error in these values, estimated as about 30%, is mainly due to traces of hydroxylic impurities contained in the solvent

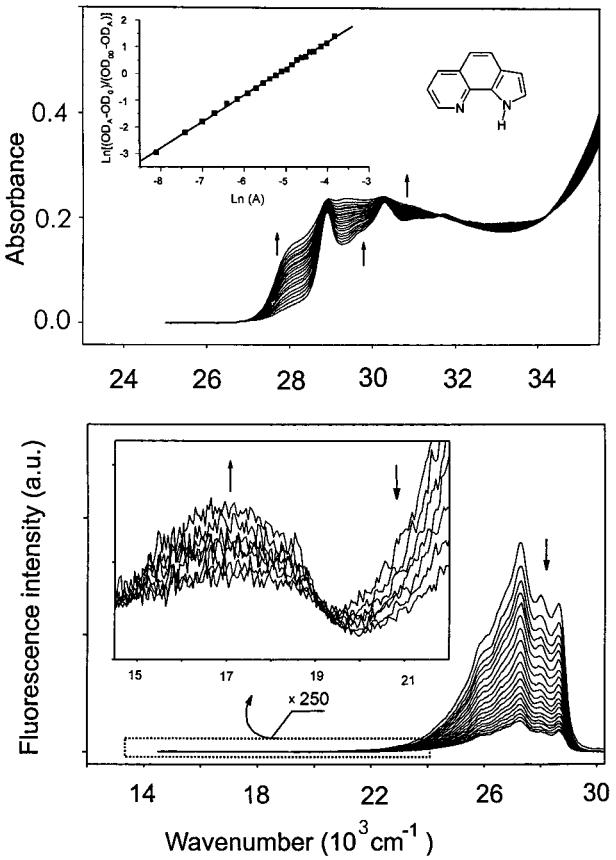

Figure 6. Titration of the solution of **PQ** in *n*-hexane with 1-butanol at 293 K. Top, changes in absorption; bottom, evolution of both fluorescence bands. The arrows show spectral changes accompanying the addition of alcohol. The alcohol concentration varied from 3.0×10^{-4} to 2.2×10^{-2} M. The insert in the top part shows the determination of the equilibrium constant and stoichiometry of the complex from the absorption data recorded at 28011 cm^{-1} (357 nm). For clarity, not all F_2 fluorescence curves are shown in the insert at the bottom.

and the sample, which leads to the appearance of similar spectral features as those obtained after adding alcohol. Therefore, careful drying of the solvent was mandatory. The value of the fluorescence quenching constant obtained for **PQ** turned out to be 4.0×10^{10} s^{-1} M^{-1}, close to the diffusion-controlled limit.

Closer examination of the changes in the emission spectra accompanying alcohol addition reveals that the model which assumes the presence of just two species, and thus, only one form of the alcohol solvate, is probably too simple. The decrease in the intensity of the F_1 fluorescence is much larger than the concomitant increase of the tautomeric emission (cf. Figure 6). Barring an explanation that assumes that the tautomeric emission is quenched by increasing amounts of alcohol (the F_2 decay times do not decrease), this finding can be explained by the presence of at least two different forms of alcohol complexes, of which only one gives rise to the phototautomer. The other form is also efficiently deactivated, but through a pathway that is different from proton transfer. Therefore, the intensity of the F_1 band decreases to a much greater extent than the observed increase of the F_2 emission. In the extreme case where just one type of complex is present and deactivated without undergoing proton transfer, only F_1 fluorescence quenching should be observed, without the appearance of the F_2 band. Actually, the situation for **PyIn-2** and **PC** seems close to that prediction, since the quantum yields of F_2 are extremely small (see Table 2).

Further arguments for the presence of two kinds of alcohol complexes, deactivated via different channels, are provided by comparison of the photophysical parameters obtained for the phototautomers with those of the *N*-methylated molecules modeling the tautomeric species. As seen from Tables 2 and 3, the room temperature decay times of tautomeric fluorescence and of the model compound emission are very similar. The quantum yields, however, are not similar, with those of the model compounds being higher. The quantum yield of the model compound fluorescence (φ_{fl}^{M}) can be expressed as the product of the radiative constant of excited-state depopulation and the fluorescence decay time:

$$\varphi_{fl}^{M} = k_r^{M}\tau^{M} \tag{2}$$

We now assume that phototautomerization may be considered an irreversible process. The expression for the quantum yield of the tautomeric emission (φ_{fl}^{T}), analogous to (2), must include *f*, the fraction of the initially excited species that end up as tautomers:

$$\varphi_{fl}^{T} = f k_r^{T}\tau^{T} \tag{3}$$

Thus

$$f = (\varphi_{fl}^{T}/\varphi_{fl}^{M})(k_r^{M}\tau^{M}/k_r^{T}\tau^{T}) \approx (\varphi_{fl}^{T}/\varphi_{fl}^{M})(\tau^{M}/\tau^{T}) \tag{4}$$

Equation 4 was obtained by assuming an equal radiative constant for the tautomeric species and its chemical model. Using eq 4 and the values from Tables 2 and 3, for **PQ** we obtain $f = 0.40$, which means that only about one-half of the excited alcohol complexes of **PQ** undergo tautomerization. The other half become deactivated in a different fashion. For **TPC** and **PC**, we obtain values of $f = 0.50$ and 0.33, respectively. Lack of exact decay times for **PyIn-2** and its tautomer model precludes the evaluation of *f* for this compound. The error in *f* may be substantial, since the quantum yield values which we use are estimated, for the worst cases, with an accuracy of ±50%. Therefore, another method was also tried, in which the values of *f* were calculated from the equation for the quantum yield of F_1 fluorescence:

$$\varphi(F_1) = f k_r\tau_{r1} + (1 - f)k_r\tau_{s1} \tag{5}$$

where k_r is the radiative rate constant, whose value was obtained from the fluorescence characteristics in acetonitrile, and τ_{r1} and τ_{s1} correspond to the lifetime of the rapid and slower decay, respectively. For the latter, the values from Table 2 were used. For the former, $\tau_{r1} = 5$ ps was assumed, using the results discussed below. This led to values of $f = 0.46$, 0.77, and 0.21 for **PQ**, **TPC**, and **PC**, respectively. While the numerical values of *f* are only semiquantitive, they indicate that the fraction of molecules which are able to phototautomerize varies along the series. It is about 50% in **PQ** and **TPC**, and much less in **PC**. The smaller fraction of tautomerizing species in **PC** is in accord with the observation that photoreaction in this molecule can be arrested at low temperature. Since the same behavior is observed in **PyIn-2**, we conclude that in this molecule the value of *f* must also be rather small. Finally, we recall that in **DPC** we have estimated *f* to be very high, about 0.97, which is approximately twice as high as the values obtained for **PQ** and **TPC**. Interestingly, **DPC** possesses twice as many hydrogen bond acceptor centers as these two molecules.

A possible assignment of the two types of alcohol complexes would attribute the fraction capable of undergoing tautomerization to 1:1 cyclic, doubly hydrogen-bonded complexes. The other fraction would include solvates of various geometries and

stoichiometries, which share a common feature: the inability to tautomerize. It was somewhat surprising to find that the latter fraction can be quite large, even at room temperature. One would have expected that thermally activated solvent reorientation, leading to phototautomerization, is possible, by analogy with the process occurring in **7AI** in several hundred picoseconds (depending on the alcohol).[17] However, time-resolved kinetic studies, which will be described in detail elsewhere,[42] led to the detection of a faster nonradiative process. Femto- and picosecond fluorescence measurements revealed at least two components in the decay of the high-energy emission. The faster decay (3−6 ps) could be correlated with the rise time of the tautomeric fluorescence. On the other hand, the slower decay component of F_1 (tens of picoseconds, varying somewhat in different alcohols) had no counterpart in the F_2 rise. Thus, direct evidence was provided for two different structures emitting the "normal" F_1 fluorescence. One of them is able to undergo tautomerization, while the other is deactivated via a different channel, internal conversion to the ground state. Even though the deactivation does not lead to a phototautomer, it must be related to hydrogen bonding with the alcohol, since in aprotic solvents, both polar and nonpolar, the monoexponential decay is nearly an order of magnitude slower. Moreover, because rapid internal conversion occurs only in chromophores capable of forming cyclic, doubly hydrogen-bonded arrays, the excited state relaxation path that starts from the point on the potential energy surface corresponding to an initially excited "blocked" complex must involve both tautomerization and radiationless deactivation. In other words, the complex is trying to achieve a cyclic structure, but cannot reach it, because it gets deactivated along the way. The excited complexes which were already cyclic in the ground state avoid the region of rapid deactivation. They undergo tautomerization with a rate about an order of magnitude faster than internal conversion. Interestingly, the tautomerization rate does not seem to depend much on temperature and solvent viscosity, whereas these parameters are crucial to the rate of internal conversion. The very fast rate of excited state double proton transfer provides another argument for the cyclic structure of the complex which is well "prepared" for the reaction.

Deuteration of the alcohol hydroxyl group does not greatly influence the emission properties. The relative intensities of **PQ** and **TPC** were found to be practically unchanged in normal and deuterated ethanol at 293 K. The fluorescence lifetimes were also similar. This again confirms that the relaxation coordinate is not directly related to proton transfer. At this stage we cannot exclude, however, that the short F_1 decay time, which is attributed to tautomerization in cyclic complexes, is not influenced by deuteration. Measurements with higher temporal resolution are under way to address this problem.[42]

An intriguing question is why, in a series of similar compounds with identical topology of hydrogen bonding sites, only some members are able to form cyclic ground state complexes in bulk alcohol. Distinction between the two classes becomes particularly clear at low temperatures. We have previously shown that the spectral behavior of **DPC** in rigid alcohol glasses reveals the existence of both kinds of solvates: cyclic ones, which undergo tautomerization, and the "blocked" species, which emit a "normal" fluorescence and phosphorescence.[40] In contrast, no evidence for cyclic structures was found at low temperatures for pyridylindoles, which showed the same emission characteristics as in aprotic solvents. Of the three new molecules studied in this work, **PQ** and **TPC** revealed tautomeric fluorescence at low temperatures, thus pointing to the presence of cyclic complexes, whereas **PC** did not. Figure 7 shows the emission spectra of **TPC** at 123 and 77 K. At 77 K, the F_2 fluorescence was obscured by the phosphorescence, lying at somewhat higher energies. This situation is analogous to that found for **DPC**, where the F_1 band and phosphorescence were assigned to noncyclic species, whereas the F_2 fluorescence was attributed to the product of excited state double proton transfer, occurring in cyclic complexes.[40] The F_2 band was easier to detect at low temperatures in **DPC** than in **PQ** and **TPC**, because of the larger F_2/F_1 intensity ratio and better spectral separation between the F_2 and phosphorescence bands in **DPC**. In the case of **PQ** and **TPC**, the presence of F_2 at 77 K could be detected by kinetic measurements, which revealed a decay time of about 0.5 ns, characteristic of the tautomer and quite different, at this temperature, from the decay time of the F_1 emission. The latter was found to be 7.8 ns, meaning that the species emitting the F_1 fluorescence cannot be a precursor to the F_2 band. This observation provides yet another argument for the presence of two different ground state forms of alcohol solvates.

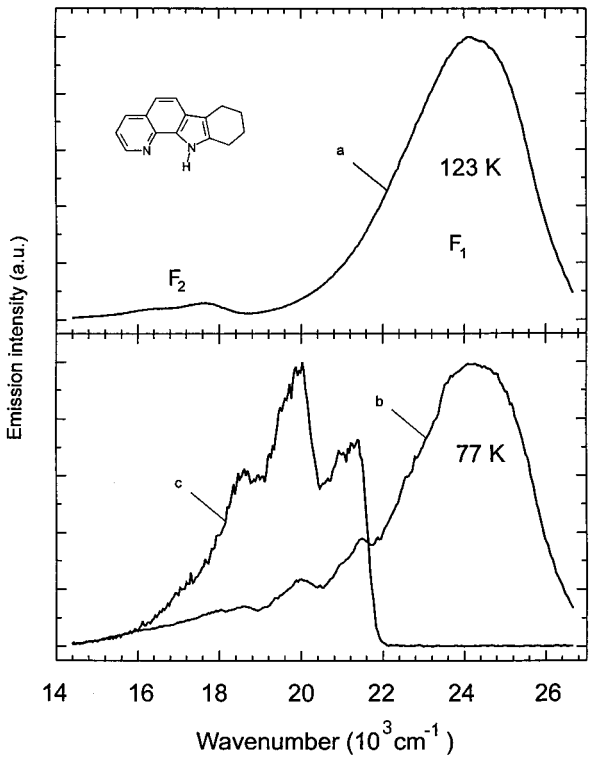

Figure 7. Emission of **TPC** in 1-propanol at 123 (top) and 77 K (bottom). Curves a and b represent total luminescence, whereas curve c corresponds to phosphorescence, separated by choppers.

Attempts to reproduce differences in the ground-state structure of the alcohol complexes by quantum mechanical calculations were not successful. Calculations of 1:1 complexes led to cyclic species for all the systems studied, with very similar heats of formation, 8.7 ÷ 9.2 kcal/mol (RHF/6-311G(d,p)). Also the ground-state values of the effective valence electron potentials on the nitrogen centers were very similar, as shown in Table 1.

It seems that better predictions can be obtained by taking into account both the chromophore characteristics and the collective properties of the bulk alcohols. Recent work by Mente and Maroncelli[18] is a promising step in that direction. Using Monte Carlo and molecular dynamics calculations, they demonstrated, in agreement with experiments, that in bulk alcohols no cyclic structures are formed between **7AI** or **1AC** and alcohols, whereas for **DPC** such species can arise. Encouraged by these results, we have performed molecular dynamics simulations of the ground-state structure of alcohol solvates for

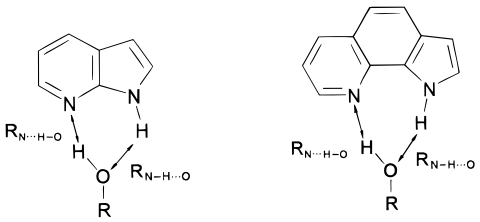

Figure 8. Hydrogen-bonding distances in **7AI** and **PQ** monitored by molecular dynamics calculations.

the compounds presently under investigation. In Figures 8 and 9 we compare the hydrogen-bonding properties of **7AI** and **PQ**, simulated first for *n*-hexane solutions with one methanol molecule added and then for bulk methanol solvent. The results obtained for **7AI** are essentially similar to those reported by Maroncelli. At low alcohol concentration, formation of a cyclic, 1:1 doubly hydrogen-bonded complex is expected. But in bulk alcohol, such structures are essentially no longer present. Instead, formation of two hydrogen bonds with two different alcohol molecules is preferred. The results obtained for **PQ** are similar to those for **7AI** at low alcohol concentration. Again, formation of a cyclic complex is predicted. However, in contrast to **7AI**, such complexes persist also in bulk methanol, along with other species, such as 1:2 complexes. Thus, the experimentally observed differences between **7AI** and **PQ** are reproduced by simulations, similar to the previously obtained results for **DPC**.[18] We have also performed simulations for **PyIn-2**, a molecule with less proclivity to form cyclic complexes. The results are shown in Figure 10. Both 1:1 cyclic and 1:2 species are predicted, similarly as for **PQ**. However, quantitative differences can be noticed. In contrast to the results obtained for **PQ** (Figure 9b), and in nice agreement with experimental results, the height of the maximum corresponding to the 1:1 cyclic species is much lower in **PyIn-2** than the height of the other two maxima, corresponding to noncyclic structures.

We have estimated the relative fractions of cyclic and noncyclic species for **7AI**, **PQ**, and **PyIn-2** in bulk methanol. For that purpose, we first integrated the distribution of $R_{NH\cdots O}$ and $R_{N\cdots HO}$ distances for values smaller than 4 Å, i.e., considering only the first solvation shell. The integration was then repeated for $R_{NH\cdots O}$ and $R_{N\cdots HO}$ simultaneously smaller than 2.5 Å. The latter value was thus used for the definition of the cyclic complex. This procedure yielded values of 1%, 13%, and 68% as the fractions of the cyclic species for **7AI**, **PyIn-2**, and **PQ**, respectively.

The difference between the behavior of alcohol solutions of **PQ** on one hand and **7AI** on the other may be traced to the ease of formation of cyclic hydrogen bonds. It can be seen in Figure 8 that the two bonds involving **PQ** are more linear than those involving **7AI**. Therefore, in bulk alcohol, the formation of separate hydrogen bonds to the two centers and alcohol−alcohol hydrogen bonding interactions in the vicinity of the solute are more probable in **7AI**. The differences among the presently studied molecules are of more subtle and quantitative nature, since the topology of the double hydrogen bond is very similar along the series.

Finally, it can be noted from Figure 9b that in a cyclic complex formed by **PQ** in bulk methanol, the distribution of

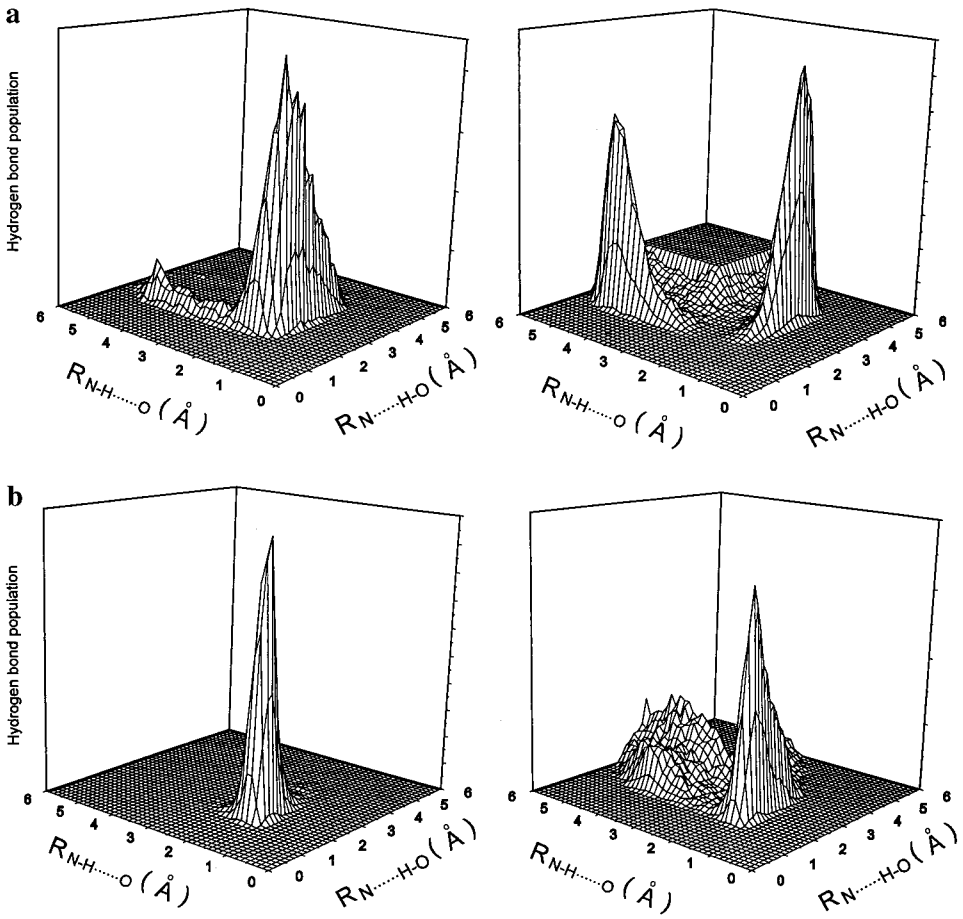

Figure 9. Distribution of $R_{NH\cdots O}$ and $R_{N\cdots HO}$ distances in **7AI** (a) and **PQ** (b). Left, *n*-hexane solutions with one methanol molecule added, resulting in cyclic, doubly hydrogen-bonded complexes. Right, simulations for bulk methanol. In the latter, the plot was cut for distances larger than 4.2 Å, to improve the visibility of the contribution due to hydrogen bonds.

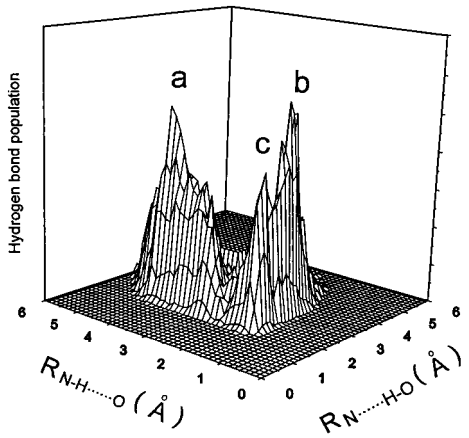

Figure 10. Distribution of $R_{NH\cdots O}$ and $R_{N\cdots HO}$ distances in **PyIn-2**. The maxima a and b represent noncyclic hydrogen bonded species, while the maximum c corresponds to a cyclic, doubly hydrogen-bonded complex.

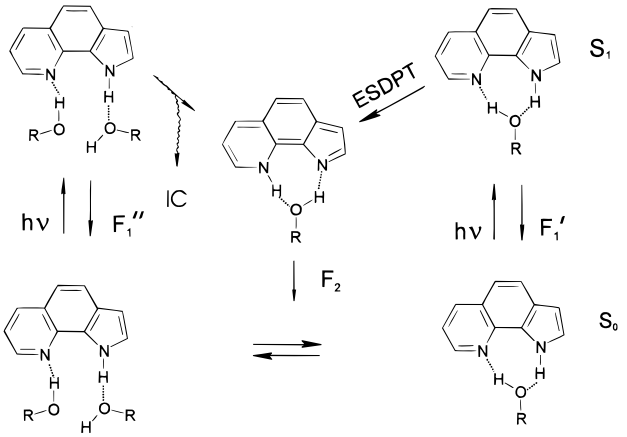

Figure 11. General scheme of ground-state equilibria and photophysical processes occurring in alcohol solvates.

NH···O distances is much narrower than that of N···HO, which implies that the bonding to the NH group is much less "loose" than bonding to the pyridine nitrogen. This result is in agreement with our earlier finding that the spectral changes observed while titrating nonpolar solutions are mostly due to the formation of NH···X hydrogen bonds, and may be observed also when a proton acceptor X, other than alcohol, is used, e.g. pyridine or DMSO.[37,38]

4. Conclusions

Spectral and theoretical studies of a series of bifunctional molecules possessing hydrogen-bonding donor and acceptor sites resulted in a model that explains the mechanisms of rapid excited-state deactivation in alcohol solutions in terms of the ground-state structure of alcohol complexes (Figure 11). The molecules which are present in the ground state in the form of cyclic hydrogen-bonded complexes with alcohol undergo, after electronic excitation, a rapid photoinduced double proton-transfer reaction. The rate of this process, of the order of 10^{11} s^{-1}, is not greatly influenced by temperature or solvent properties, such as viscosity. On the other hand, these parameters determine the rate and efficiency of another channel of excited-state deactivation, internal conversion to the ground state, occurring in noncyclic solvates. The rate of this process, higher than 10^{10} s^{-1} at room temperature, becomes negligible in low-temperature rigid alcohol glasses. Obviously, internal conversion is controlled by solvent relaxation around the excited chromophore.

Figure 11 implies that the "normal" emission, F_1, may not be homogeneous in alcohols. At least two components are expected, labeled F_1' and F_1'', corresponding to fluorescence from cyclic and noncyclic solvates, respectively. The two components should respond differently to changes in solvent viscosity, polarity, and temperature. Indeed, the nonhomogeneous character of F_1 has been recently observed.[42]

The photophysical behavior of the molecules investigated in this study appears to be quite different from that of **7AI**, a classical model of photoinduced double proton transfer. The tautomerization rate was found to be 2 orders of magnitude faster than in **7AI**, which lacks the alcohol complexes "prepared" for tautomerization. In turn, the mechanism of proton transfer occurring in **7AI**, involving solvent relaxation around the excited chromophore, could not be realized, because of another, faster deactivation channel, $S_1 \rightarrow S_0$ internal conversion. Taken together, the systems studied in this work on the one hand and **7AI** and **1AC** on the other, provide an interesting class of compounds in which the same type of chemical reaction is governed by various mechanisms, both intra- and intermolecular, and for which the origin for the excited-state reactivity can be traced back to the ground-state properties. This feature makes these systems very good models for comparative theoretical studies which attempt to establish the links between structure and reactivity.

Acknowledgment. This work has been financed by the US−Polish Maria Skłodowska-Curie Joint Fund II (grant No. 97-305) and by a grant from the Foundation for Polish Science ("Fastkin" program). The technical assistance of G. Orzanowska and A. Zielińska is gratefully appreciated. We thank Dr J. Karolczak from the Ultrafast Laser Spectroscopy Laboratory at the A. Mickiewicz University, Poznań, Poland for help in the lifetime measurements. We are grateful to Y. Stepanenko for help in the analysis of the results of MD calculations. F.W. and R.P.T. thank the Robert A. Welch Foundation (E-0621) and the National Science Foundation (CHE-9714998) for financial support of this work.

JA991817Z